

## Evaluation of 3D structures fabricated with two-photon-photopolymerization by using FTIR spectroscopy

Klaus Cicha, Zhiquan Li, Klaus Stadlmann, Aleksandr Ovsianikov, Ruth Markut-Kohl, Robert Liska, and Jürgen Stampfl

Citation: [Journal of Applied Physics](#) **110**, 064911 (2011); doi: 10.1063/1.3639304

View online: <http://dx.doi.org/10.1063/1.3639304>

View Table of Contents: <http://scitation.aip.org/content/aip/journal/jap/110/6?ver=pdfcov>

Published by the [AIP Publishing](#)

---

### Articles you may be interested in

[Development of functional sub-100 nm structures with 3D two-photon polymerization technique and optical methods for characterization](#)

[J. Laser Appl.](#) **24**, 042004 (2012); 10.2351/1.4712151

[Fabrication of three-dimensional calixarene polymer waveguides using two-photon assisted polymerization](#)

[Appl. Phys. Lett.](#) **90**, 033511 (2007); 10.1063/1.2430480

[Ultraprecise microreproduction of a three-dimensional artistic sculpture by multipath scanning method in two-photon photopolymerization](#)

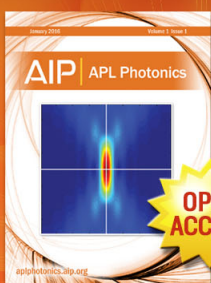
[Appl. Phys. Lett.](#) **90**, 013113 (2007); 10.1063/1.2425022

[Three-dimensional photonic crystal structures achieved with two-photon-absorption photopolymerization of resin](#)

[Appl. Phys. Lett.](#) **74**, 786 (1999); 10.1063/1.123367

[APL Photonics](#)

---



Launching in 2016!  
The future of applied photonics research is here

**AIP** | **APL Photonics**

# Evaluation of 3D structures fabricated with two-photon-photopolymerization by using FTIR spectroscopy

Klaus Cicha,<sup>a)</sup> Zhiquan Li, Klaus Stadlmann, Aleksandr Ovsianikov, Ruth Markut-Kohl, Robert Liska, and Jürgen Stampfl

*Institute of Materials Science and Technology, Vienna University of Technology, Favoritenstrasse 9–11, 1040 Vienna, Austria*

(Received 15 June 2011; accepted 10 August 2011; published online 26 September 2011)

Two-photon-induced photopolymerization (2PP) has gained increased interest due to the capability of manufacturing three-dimensional structures with very high feature resolution. To assess the suitability of photopolymer systems for 2PP, methods have to be developed that allow a screening of the efficiency of monomer-initiator combinations in the context of high throughput, large processing window and geometric quality of the final parts. In this paper, a method for evaluating 2PP structures is described. For this purpose, the double-bond conversion of fabricated 2PP structures was measured giving quantifiable results about the efficiency of the photoinitiator. The method is based on local measurement of the double-bond conversion of the photopolymer using a microscope in combination with infrared spectroscopy. The obtained double-bond conversion is a measure for the efficiency of the photopolymer system (initiator in combination with monomer), and thus allows to compare different photopolymers in a quantitative way. Beside this evaluation of 2PP structures, fabrication of complex 3D structures was done to determine the limits of the 2PP technology for miscellaneous components. © 2011 American Institute of Physics.  
[doi:[10.1063/1.3639304](https://doi.org/10.1063/1.3639304)]

## I. INTRODUCTION

The interest in two-photon polymerization<sup>1–4</sup> has highly increased during the last years because of its various potential applications such as in the field of mechanical, electronic, and optical microdevices,<sup>5–7</sup> polymer based optical waveguides,<sup>8–10</sup> optical data storage,<sup>11,12</sup> biomedical applications,<sup>13,14</sup> and the like. Two-photon-induced photopolymerization (2PP) is an additive manufacturing technology (AMT)<sup>15</sup> where a two-photon absorption by a photoinitiator induces photochemical reaction resulting in a resin cured inside the focal point of a pulsed laser beam. With this unique process, it is possible to produce complex 3D structures with feature sizes below the diffraction limit of the utilized light source. Malinauskas *et al.*<sup>16</sup> showed that in addition to two-photon absorption, a thermally induced reaction might occur under special conditions. Li *et al.*<sup>17</sup> and Pucher *et al.*<sup>18</sup> proved by variation of the photoinitiator, and their concentration that the photoinitiator is one of the key components to initiate the polymerization.

For material research and development, a reproducible evaluation system is indispensable to compare different materials and/or material components. Due to the small sample size (micrometer scale) and long fabrication times (typical federate between 100  $\mu\text{m/s}$  and 1 mm/s)<sup>19,20</sup> traditional material testing methods (e.g., tensile test, notch-bar impact test, hardness test) cannot be used for 2PP structures. Khripin *et al.*<sup>21</sup> described a method to measure the elastic modulus of micro-cantilevers fabricated with a mask-directed multiphoton lithography approach by using atomic force microscopy

(AFM). Although this method is technologically very interesting, the necessary expenses and efforts are rather high. Therefore other and more applicable methods had to be created to provide a solid base for investigations on the two-photon polymerization process.

In literature, the two-photon absorption (TPA) cross section is the most common value to evaluate TPA chromophores.<sup>18,22,23</sup> There are many different possibilities to measure the TPA cross section, such as nonlinear transmission,<sup>24</sup> up-converted fluorescence emission,<sup>25</sup> transient absorption,<sup>26</sup> four-wave mixing,<sup>27</sup> and z-scan analysis.<sup>22</sup> The advantages of z-scan measurements are the sensitivity, relatively low cost, and ease in performance. On the other hand, there are some drawbacks—this method is rather time consuming, and a precise laser setup is indispensable for achieving reliable results as an outcome of the fitting calculations. Several modifications of the classic z-scan setup were done to cope with the preceding disadvantages.

Nevertheless, the major drawback of this method that cannot be compensated by modifications of the setup is the missing correlation of absorption and efficiency of the photoinitiator. The TPA cross section is an indication of the amount of energy that can be absorbed by the initiator molecule in a two-photon process. A large TPA cross section indicates that a large amount of energy has been absorbed. Unfortunately large energy absorption is not necessarily an indication of an efficient initiation by radicals. The absorbed energy can lead to fluorescence or can be converted to thermal energy. In both cases, the energy is lost and does not contribute to generating radicals. This means that the measurement of TPA cross sections alone is not sufficient for assessing the efficiency of two-photon initiators.

<sup>a)</sup>Author to whom correspondence should be addressed. Electronic mail: [klaus.cicha@tuwien.ac.at](mailto:klaus.cicha@tuwien.ac.at).

As UV-Vis spectroscopy and TPA cross section measurements only describe the efficiency in population of the excited state, information on the formed radicals are essential. Usually time resolved ESR, chemically induced dynamic nuclear polarization (CIDNP), or laser flash photolysis is used to identify radical species. Due to the low excited volume and the low radical concentration, these methods were not suitable up to now to study kinetics and mechanisms in radical two-photon polymerization. Under one-photon excitation conditions, methods like Photo-differential scanning calorimetry (DSC), RT-FTIR or photorheology are used to follow the curing kinetics and the double-bond conversion. Unfortunately, these methods are again not suitable to follow the photocuring process under two-photon conditions as the polymerizing volume is too low. Beside this, the use of one-photon measurements may lead to some inaccuracy because for centrosymmetric molecules [like the photoinitiator 2,7-bis ((4-dibutylamino)phenyl) ethynyl)-9 H-fluoren-9-one (B3FL)], there is no direct correlation between the one-photon absorption (OPA) maxima and the TPA maxima ( $\lambda_{\text{OPAmax}} \neq 2 \times \lambda_{\text{TPAmax}}$ ).<sup>28</sup> This is caused by the fact that for centrosymmetric molecules, a OPA-allowed excited state cannot be reached directly by TPA (usually the lowest TPA-allowed state has a higher energy level than the OPA-allowed).<sup>28–30</sup> Therefore other approaches are described in literature to characterize the efficiency of the initiator by looking at the polymerized specimens.

Several parameters can be investigated to evaluate the 2PP process and/or the materials. Valuable parameters characterizing the process are the maximum structuring speed and the fabrication window for a certain laser power. Among the parameters characterizing the quality of produced structures are the dimensions of the voxel and the achievable resolution. The resolution is not only influenced by the process environment but additionally by the material. The focus of research was mainly related to the efficiency of the photoinitiator because most commercially available one-photon initiators have only poor efficiency for two-photon polymerization. Only little work was done on characterization of fabricated 2PP structures. In this work, the double-bond conversion (DBC) of fabricated 2PP structures was detected by using FTIR spectroscopy, giving a quantifiable measure to compare different systems against each other. The presented method therefore provides a reliable screening of initiator-monomer systems.

## II. EXPERIMENTAL SECTION

### A. 2PP setup

Fabrication of the microstructures was done using a standard 2PP setup. Starting with the Ti-sapphire laser (max. power: 450 mW) creating 73 fs pulses with 80 MHz repetition rate the near-infrared laser beam (wavelength  $\lambda = 793$  nm) passes through an acousto-optic-modulator (AOM). The AOM shutters and diffracts the laser beam—only the first order wave is used for polymerization. The laser power can be adjusted by a rotatable  $\lambda/2$  waveplate and the subsequent polarizing depending beam-splitter. These two optical components divide the laser beam depending on

the polarization—therefore the laser power reaching the sample can be adjusted. Laser power not allowed to reach the sample is led to a Coherent FieldMax II powermeter. The X and Y movements are realized by high precision air bearing axes carrying optical components like optical mirrors, the CCD camera, and the microscope objective for focusing the laser beam.

While the X and Y movements are done by the moving laser beam, the Z movement is realized by a vertical mounted and weight-compensated air bearing axis carrying the sample. The CCD camera uses the same microscope objective as used for focusing the laser beam. Thus the fabrication process can be live monitored. The axes are mounted on a hard stone housing placed on an optical table with an air-friction damping. Therefore the complete setup is insensitive to vibrations.

### B. Material

For the experiments, a photopolymerizable monomer and two different photoinitiators were used. The monomer was a 1:1 mixture (wt. %) of ethoxylated (20/3)-trimethylolpropanetriacrylate (ETA, Sartomer 415) and trimethylolpropane triacrylate (TTA, Genomer 1330). This monomer was used because of good results obtained in preliminary tests.<sup>17</sup>

Two photoinitiators were screened in combination with above mentioned resin. For sample “A,”  $6.3 \times 10^{-6}$  mol photoinitiator/g resin of B3FL was added as photoinitiator. E,E-1,4-bis[4'-(*N,N*-di-*n*-butylamino) styryl]-2,5-dimethoxybenzene (R1) was used as photoinitiator for formulation “B” (again  $6.3 \times 10^{-6}$  mol photoinitiator/g resin).

The photoinitiator B3FL (Ref. 17) is based on the molecular structure of B3 K (Ref. 18) containing triple bonds and a cross conjugated D- $\pi$ -A- $\pi$ -D lead structure. Compared to R1, which is a very potent two-photon initiator well known from literature,<sup>17,18,22,31</sup> B3FL contains fluorenone as acceptor in the central part of the  $\pi$  bridge. The introduction of an aromatic ketone with a stereo rigid carbon frame not only facilitates the intramolecular charge transfer process but also extends the conjugation length of the whole  $\pi$  system, which is critical in enhancing the TPA cross section. It is worth mentioning that compared to R1, which exhibits strong fluorescence, the triple bond containing ketone-based photoinitiator show very weak emission. For TPA, photoinitiators with low fluorescence quantum yields are preferred as this is a requirement for a high population of the triplet state (triplet quantum yield), which is usually the active state of the initiators producing radicals or ions for initiating the polymerization. The good suitability of B3FL for 2PP could be seen in the z-scan results (Ref. 17)—R1:  $\sigma_{\text{TPA}} = 328$  GM; B3FL:  $\sigma_{\text{TPA}} = 440$  GM (1 GM =  $10^{-50}$  cm<sup>4</sup> s photon<sup>−1</sup> molecule<sup>−1</sup>). Photo-DSC measurements showed that B3FL is very inert to one-photon irradiation, which implied its excellent one-photon stability for daily use.

### C. Sample preparation

The building parameters were set to values leading to fully solid and cube-like structures (size 50  $\mu\text{m}$ ; period 1  $\mu\text{m}$ ; layer distance 1  $\mu\text{m}$ ; 30 layers). For formulation A,



the laser power and structuring speed were varied—3 mW intervals for the laser power and 100  $\mu\text{m/s}$  intervals for the structuring speed (100  $\mu\text{m/s}$  to 800  $\mu\text{m/s}$ ). Making the structures using formulation B, the geometry parameters were chosen same as for formulation A; laser power was varied again but the structuring speed was held constant at 400  $\mu\text{m/s}$ .

As glass absorbs IR light with the wavelength used for FTIR spectroscopy, the woodpile structures were fabricated on a potassium bromide plate. Additionally due to the numerous different samples (changed laser power and structuring speed combinations), traditional IR-sample preparation (high-pressure vacuum molding of potassium bromide and material—simultaneous grounded) is not possible. Therefore a pure potassium bromide plate was molded and fixed on a substrate that can be mounted in the 2PP setup. On this potassium bromide plate, an array of woodpile structures was fabricated. Potassium bromide (KBr) shows hygroscopic behavior. Therefore direct contact of the KBr plate with fluids (monomer, development solvents) has to be restricted to a minimum. The complete building process took 9 h (depending on the size of the array), removing of the residual monomer (rinsing the sample with ethanol) 15 min. By choosing a suitable background spectrum, the influence of the KBr plate on the IR spectrum can be compensated.

### III. RESULTS AND DISCUSSION

#### A. Measurement of the double-bond conversion using FTIR spectroscopy

The method relies on measuring the double-bond conversion (DBC) of the structured polymers. The DBC gives a good feedback about the degree of polymerization and the reactivity of the material.<sup>32</sup> The DBC was measured by means of FTIR spectroscopy using a Bruker Tensor 27 (Bruker Optics, Ettlingen, Germany) equipped with a Bruker Hyperion 1000 microscope. The scanned wave number range was 4000  $\text{cm}^{-1}$  to 600  $\text{cm}^{-1}$  with a resolution of 2  $\text{cm}^{-1}$  and 32 scans per spectrum.

As the thickness of the IR samples (2PP structure, monomer droplet, UV cured sample) could not be determined exactly, the double-bond peak had to be referenced to the carbonyl (CO) peak, which remains constant during the polymerization process because of the chemical structure of the monomer.<sup>32</sup> The change of the area of the double-bond peak can be determined and gives direct and significant information about the double-bond conversion. As can be seen from Fig. 1, for validation of the results, a IR spectrum of a one-photon polymerized material was taken, and relevant peaks (carbonyl peak at approximately 1730  $\text{cm}^{-1}$ , double-bond peak at 810  $\text{cm}^{-1}$ ) were taken into comparison to the two-photon polymerized IR spectra.

For evaluation of the DBC, the relevant peak areas were deconvoluted<sup>32</sup> using the software PEAK FIT 4. Due to the broad carbonyl peak (see Fig. 1), this step was necessary to determine the area above the baseline exactly. The broad CO peak is caused by the changing DBC over the cross section of a single scanned woodpile rod—therefore the broad carbonyl peak appears as overlay of multiple peaks. A more detailed observation of this phenomenon (high resolution DBC

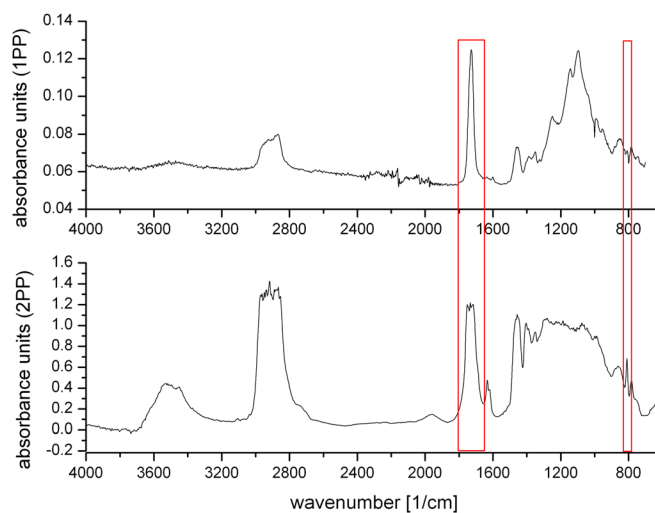


FIG. 1. (Color online) Comparison of IR-spectrums of structures produced using one-photon polymerization (1PP) and two-photon polymerization (2PP).

investigation) is necessary for confirmation. Deconvoluted peaks were taken into comparison, and the double-bond conversion was calculated.

Evaluating the 2PP structures fabricated using formulation A by measuring the DBC using FTIR-spectroscopy gives results shown in Fig. 2. The laser power showed a high influence on the double-bond conversion. First structures could clearly be seen at 23 mW (laser power measured before passing the 20 $\times$  magnification microscope objective with NA = 0.8)—the lower threshold energy level (LTEI)—at this laser-power level a DBC of approximately 57% was determined (depending on the structuring speed). Advancing the laser power to 115% of the LTEI increased the DBC level up to 65%. At the subsequent increments, the DBC increased only 1 to 2 percentage points (or even less). After 175% of the LTEI, the DBC level remains nearly constant—further increase of the laser power does not lead to higher DBC. The structuring speed influenced the DBC only at low laser intensities—an increase in laser power led to a kind of structuring speed independency. This is only correct for structuring speeds in the range of 100  $\mu\text{m/s}$  to 800  $\mu\text{m/s}$

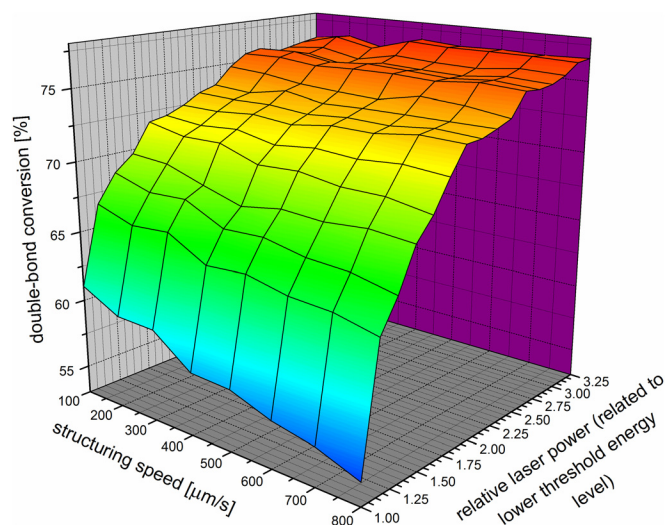


FIG. 2. (Color online) Double-bond conversion of formulation A.

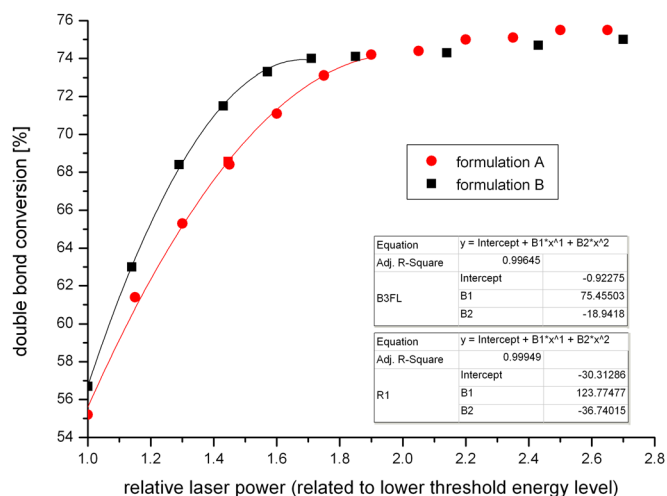


FIG. 3. (Color online) DBC comparison of formulations with different photoinitiators and 2nd order fitting function of rising DBC values.

(as it was used for the fabrication process—unfortunately higher structuring speeds in combination with small structure dimensions are at this point in time not possible). It is highly assumed that rising structuring speeds at constant laser power would lead to a decrease of the DBC—even at laser energies that showed no influence on the structuring speed in this experiment. Further investigations are necessary to confirm this assumption.

The successive dots in Fig. 3 show the DBC comparison of formulations A and B. The overall development of the DBC curves for these two material systems is comparable. But it can easily be seen that the DBC of formulation B increases faster than the DBC of formulation A. This indicates that B seems to have a more abrupt on/off (polymerization) behavior. Taking mechanical stability into account, high DBC with a laser power close to the LTEL is favored. This would give high resolution micro-structures with high mechanical stability (due to adequate cross linking).

## B. DBC fitting function

The rising DBC level seems to follow some typical curve progression—a nonlinear absorption behavior is well known from literature.<sup>1,33–35</sup> The number of photons absorbed in a certain time period is described by Lin *et al.*<sup>34</sup> as

$$\frac{dn_{\text{photon}}}{dt} = \sigma \times N \times \left( \frac{I}{h \times \nu} \right)^2 \quad (1)$$

where  $N$  is the number (concentration) of absorbing molecules,  $\sigma$  is the two-photon absorption cross section and  $(I/(h \times \nu))$  is the photon flux of the light source. Leatherdale<sup>35</sup> described the rate of generation of polymerization initiating species  $R_{2i}$  proportional to

$$R_{2i} = \frac{1}{2} \times \frac{g_p}{\tau \times f} \times \left( \frac{\lambda}{h \times c} \right) \times \frac{P^2}{A^2} \times N \times \delta \times \phi \quad (2)$$

where  $P$  is the average power,  $\tau$  is the pulse length,  $f$  is the laser repetition rate,  $\lambda$  is the excitation wavelength,  $h$  is Planck's constant,  $c$  is the speed of light,  $A$  is the laser spot size,  $N$  is the concentration of two-photon absorbing chromophores,  $\delta$  is the two-photon absorption cross section,  $\phi$  is the quantum efficiency for conversion of excited states to polymerization initiating species, and  $g_p$  is a parameter determined by the precise shape of the laser pulse. From Equation (1) and (2) it follows that the laser intensity  $I$ , respectively the laser power  $P$ , influence the two-photon absorption and polymerization process by the power of two.

The straight line in Fig. 3 shows the second order fitting function of the DBC results. Only the first values of each curve were taken into account as these are the regions where changes of the DBC level can be seen. Calculation of the coefficient of determination ( $R^2$ ) of the second order polynomial fitting functions proved the direct dependency of the DBC to the nonlinear two-photon absorption behavior.

## C. Complex 3D structures

Using the optimized fabrication parameters described in the previous sections, different 3D structures were fabricated using 2PP. Figure 4 shows free-standing high resolution structures fabricated without the need of any support material fixing the structure during the building process. The high potential of this technology, producing parts applicable for various future applications e.g., mechanical, electronic, and optical microdevices can easily be imagined.

## IV. CONCLUSIONS

A new and quantifiable method for evaluation of structures fabricated by two-photon polymerization (2PP) was established. Recording of local IR spectrums of fabricated 2PP structures was done the first time—subsequent calculation of the double-bond conversion gave further knowledge

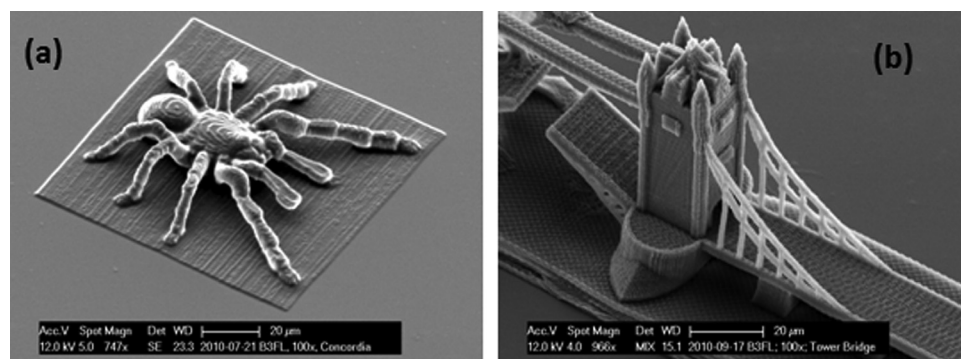


FIG. 4. Complex 3D structures.

of the polymerization process. Starting with a laser power close to the LTEL leads to a DBC level of approximately 56%. Subsequent (increasing) laser-power steps lead to sharply rising DBC values reaching a steady state maximum of 75%. Beside this as a second rather surprising result, the influence of the structuring speed on the DBC could only be observed at laser power levels close to the LTEL. After reaching higher energy levels, the DBC remained constant and showed a structuring speed independency in the used range of structuring speeds. The method allows screening of photopolymer systems regarding their suitability for 2PP and gives a measure to quantitatively compare different systems against each other. The time-consuming peak deconvolution and calculation step is the major drawback of this approach.

Beside the evaluation of 2PP structures, fabrication of complex 3D structures was done to determine the limits of the 2PP technology for miscellaneous components. Different model geometries were structured, and the results indicate the capabilities of 2PP for the fabrication of complex 3D structures. Feature size down to 700 nm using structuring speeds from 50  $\mu\text{m/s}$  to 500  $\mu\text{m/s}$  can be achieved. Free standing structures built without supporting material are possible as well as microstructures with high aspect ratios.

## ACKNOWLEDGMENTS

The financial support by the Austrian Research Agency FFG under Contract No. 819718 (research project cluster ISOTEC) is greatly acknowledged. Furthermore the authors thank Jan Torgersen (Vienna University of Technology) for his valuable input and discussions and Andreas Mautner (Vienna University of Technology) for FTIR measurements of one-photon-polymerized materials.

<sup>1</sup>H.-B. Sun and S. Kawata, *ChemInform* **36**, 169 (2004).

<sup>2</sup>H.-B. Sun and S. Kawata, *J. Lightwave Technol.* **21**, 624 (2003).

<sup>3</sup>S. Wu, J. Serbin, and M. Gu, *J. Photochem. Photobiol., A* **181**, 1 (2006).

<sup>4</sup>K.-S. Lee, R. H. Kim, D.-Y. Yang, and S. H. Park, *Prog. Polym. Sci.* **33**, 631 (2008).

<sup>5</sup>H.-B. Sun, S. Matsuo, and H. Misawa, *Appl. Phys. Lett.* **74**, 786 (1999).

<sup>6</sup>C. Schizas, V. Melissinaki, A. Gaidukeviciute, C. Reinhardt, C. Ohrt, V. Dedoussis, B. N. Chichkov, C. Fotakis, M. Farsari, and D. Karalekas, *Int. J. Adv. Manuf. Technol.* **48**, 435 (2009).

<sup>7</sup>S.-H. Park, D.-Y. Yang, and K.-S. Lee, *Laser Photon. Rev.* **3**, 1 (2009).

<sup>8</sup>R. Infuehr, N. Pucher, C. Heller, H. Lichtenegger, R. Liska, V. Schmidt, L. Kuna, A. Haase, and J. Stampfl, *Appl. Surf. Sci.* **254**, 836 (2007).

<sup>9</sup>V. Satzinger, V. Schmidt, L. Kuna, C. Palfinger, R. Infuehr, R. Liska, and J. R. Krenn, *Proceedings of SPIE* **6992**, 699217 (2008).

<sup>10</sup>K. Stadlmann, K. Cicha, J. Kumpfmüller, V. Schmidt, V. Satzinger, J. Stampfl, and R. Liska, in *Proceedings of LPM* (Stuttgart, Germany 2010).

<sup>11</sup>D. A. Parthenopoulos and P. M. Rentzepis, *Science* **245**, 843 (1989).

<sup>12</sup>B. H. Cumpston, S. P. Ananthavel, S. Barlow, D. L. Dyer, J. E. Ehrlich, L. L. Erskine, A. A. Heikal, S. M. Kuebler, I.-Y. S. Lee, D. McCord-Maughon, J. Qin, H. Rockel, M. Rumi, X.-L. Wu, S. R. Marder, and J. W. Perry, *Nature* **398**, 51 (1999).

<sup>13</sup>A. Ovsianikov, A. Deiwick, S. Van Vlierberghe, P. Dubruel, L. Möller, G. Dräger, and B. Chichkov, *Biomacromolecules* **12**(4) pp. 851–858 (2011).

<sup>14</sup>A. Ovsianikov, S. Schlie, A. Ngezahayo, A. Haverich, and B. N. Chichkov, *J. Tissue Eng. Regen. Med.* **1**, 443 (2007).

<sup>15</sup>J. Stampfl, S. Baudis, C. Heller, R. Liska, A. Neumeister, R. Kling, A. Ostendorf, and M. Spitzbart, *J. Micromech. Microeng.* **18**, 125014 (2008).

<sup>16</sup>M. Malinauskas, A. Žukauskas, G. Bičkauskaitė, R. Gadonas, and S. Juodkazis, *Opt. Express* **18**, 10209 (2010).

<sup>17</sup>Z. Li, M. Siklos, N. Pucher, K. Cicha, A. Ajami, W. Husinsky, A. Rosspeintner, E. Vauthey, G. Gescheidt, J. Stampfl, and R. Liska, *J. Polym. Sci. A Polym. Chem.* **49**, 3688–3699 (2011).

<sup>18</sup>N. Pucher, A. Rosspeintner, V. Satzinger, V. Schmidt, G. Gescheidt, J. Stampfl, and R. Liska, *Macromolecules* **42**, 6519 (2009).

<sup>19</sup>G. Kumi, C. O. Yanez, K. D. Belfield, and J. T. Fourkas, *Lab. Chip.* **10**, 1057 (2010).

<sup>20</sup>Y. Liu, D. D. Nolte, and L. J. Pyrak-Nolte, *Appl. Phys. A* **100**, 181 (2010).

<sup>21</sup>C. Y. Khrupin, C. J. Brinker, and B. Kaehr, *Soft Matter* **6**, 2842 (2010).

<sup>22</sup>A. Ajami, W. Husinsky, R. Liska, and N. Pucher, *J. Opt. Soc. Am. B* **27**, 2290 (2010).

<sup>23</sup>J. Kumpfmüller, N. Pucher, J. Stampfl, and R. Liska, in *Polymer Photochemistry in Optical Applications* (Springer Publishers, New York, 2011).

<sup>24</sup>G. O. Clay, C. B. Schaffer, and D. Kleinfeld, *J. Chem. Phys.* **126**, 025102 (2007).

<sup>25</sup>C. Xu and W. W. Webb, *J. Opt. Soc. Am. B* **13**, 481 (1996).

<sup>26</sup>J. D. Bhawalkar, G. S. He, and P. N. Prasad, *Rep. Prog. Phys.* **59**, 1041 (1996).

<sup>27</sup>Q. Yang, J. Seo, S. Creekmore, G. Tan, H. Brown, S. M. Ma, L. Creekmore, A. Jackson, T. Skyles, B. Tabibi, H. Wang, S. Jung, and M. Namkung, *J. Phys.: Conf. Ser.* **38**, 144 (2006).

<sup>28</sup>M. Rumi, S. Barlow, J. Wang, J. W. Perry, and S. R. Marder, in *Photoresponsive Polymers I: Advances in Polymer Science* (Springer, Berlin, 2008), pp. 1–95.

<sup>29</sup>Y. Zhao, X. Li, F. Wu, and X. Fang, *J. Photochem. Photobiol., A* **177**, 12 (2006).

<sup>30</sup>S. Hirakawa, J. Kawamata, Y. Suzuki, S. Tani, T. Murafuji, K. Kasatani, L. Antonov, K. Kamada, and K. Ohta, *J. Phys. Chem. A* **112**, 5198 (2008).

<sup>31</sup>M. Rumi, J. E. Ehrlich, A. A. Heikal, J. W. Perry, S. Barlow, Z. Hu, D. McCord-Maughon, T. C. Parker, H. Röckel, S. Thayumanavan, S. R. Marder, D. Beljonne, and J.-L. Brédas, *J. Am. Chem. Soc.* **122**, 9500 (2000).

<sup>32</sup>C. Dworak, S. Kopeinig, H. Hoffmann, and R. Liska, *J. Polym. Sci. A* **47**, 392–403 (2009).

<sup>33</sup>M. Bass, *Handbook of Optics* (McGraw-Hill Professional, New York, 1994), Vol. 1.

<sup>34</sup>T.-C. Lin, S.-J. Chung, K.-S. Kim, X. Wang, G. S. He, J. Swiatkiewicz, H. E. Pudavar, and P. N. Prasad, in *Polymers for Photonics Applications II (Advances in Polymer Science)* (Springer, Berlin, 2003), pp. 157–193.

<sup>35</sup>C. A. Leatherdale, *Proceedings of SPIE* **5211**, 112–123 (2003).